The Plant Cell, Vol. 14, 2121–2135, September 2002, www.plantcell.org

ANTHOCYANIN1 of Petunia Controls Pigment Synthesis, Vacuolar pH, and Seed Coat Development by Genetically Distinct Mechanisms

Cornelis Spelt, Francesca Quattrocchio, Joseph Mol, and Ronald Koes[1]

Department of Developmental Genetics, Institute for Molecular Biological Sciences, Vrije Universiteit, de Boelelaan 1087, 1081 HV Amsterdam, The Netherlands

ANTHOCYANIN1 (AN1) of petunia is a transcription factor of the basic helix-loop-helix (bHLH) family that is required for the synthesis of anthocyanin pigments. Here, we show that AN1 controls additional aspects of cell differentiation: the acidification of vacuoles in petal cells, and the size and morphology of cells in the seed coat epidermis. We identified *an1* alleles, formerly known as *ph6*, that sustain anthocyanin synthesis but not vacuolar acidification and seed coat morphogenesis. These alleles express truncated proteins lacking the C-terminal half of AN1, including the bHLH domain, at an ~30-fold higher level than wild-type AN1. An allelic series in which one, two, or three amino acids were inserted into the bHLH domain indicated that this domain is required for both anthocyanin synthesis and vacuolar acidification. These findings show that AN1 controls more aspects of epidermal cell differentiation than previously thought through partially separable domains.

INTRODUCTION

The synthesis of anthocyanin pigments in floral tissue provides an excellent marker to study the differentiation of cells. Most of the structural genes that encode the ~15 enzymes required for anthocyanin synthesis and modification have been isolated (Holton and Cornish, 1995; Winkel-Shirley, 2001). By mutational analyses in Antirrhinum, Arabidopsis, maize, and petunia, several regulatory genes have been identified that are required for the tissue-specific transcription of the structural anthocyanin genes (for reviews, see Mol et al., 1998; Winkel-Shirley, 2001).

ANTHOCYANIN1 (*AN1*) of petunia encodes a basic helix-loop-helix (bHLH) protein that activates the transcription of the structural anthocyanin gene *DIHYDROFLAVONOL REDUCTASE* (*DFR*) and a putative regulatory gene (*MYB27*) whose function is unknown (Spelt et al., 2000). The *JAF13* gene encodes a bHLH protein that is homologous with DELILA (DEL) from snapdragon and R from maize (Quattrocchio et al., 1998) but functionally and evolutionary distinct from AN1 (Spelt et al., 2000). The expression of *AN1* is regulated by *AN2* and *AN4* (Spelt et al., 2000).

[1] To whom correspondence should be addressed. E-mail koes@bio.vu.nl; fax 31-20-4447155.

Article, publication date, and citation information can be found at www.plantcell.org/cgi/doi/10.1105/tpc.003772.

AN2 is expressed in the petal limb only and encodes a MYB domain protein (Quattrocchio et al., 1999) that is functionally interchangeable with C1 from maize (Quattrocchio et al., 1998) and that may be orthologous with either *TRANSPARENT TESTA2* (*TT2*) (Nesi et al., 2001) or *PRODUCTION OF ANTHOCYANIN PIGMENT1* (*PAP1*) and *PAP2* (Borevitz et al., 2000) from Arabidopsis. *AN4* encodes (or controls the expression of) a paralogous MYB protein that is expressed in anthers (C. Spelt, A. Kroon, and R. Koes, unpublished data). The activity of one or more of these transcription factors appears to be regulated post-transcriptionally by a cytosolic WD40 repeat protein encoded by *AN11* in petunia and by *TRANSPARENT TESTA GLABRA* (*TTG*) in Arabidopsis (de Vetten et al., 1997; Walker et al., 1999).

In Arabidopsis, two other transcription factors, the homeodomain protein ANTHOCYANINLESS2 (ANL2) and the zinc finger protein TT1, have been implicated in the accumulation of proanthocyanidin polymers in the seed coat (Kubo et al., 1999; Sagasser et al., 2002). However, it is unclear whether ANL2 and TT1 coregulate the anthocyanin-specific genes together with the MYB, bHLH, and WD40 proteins or control a distinct set of structural anthocyanin genes.

Although the regulatory genes mentioned above were identified initially by their role in anthocyanin synthesis, an increasing amount of evidence indicates that they control additional aspects of cell differentiation. Expression of a C1-R fusion protein in maize suspension cells causes the

activation or repression of hundreds of genes (Bruce et al., 2000), many more than are required for anthocyanin synthesis. In Arabidopsis, *ttg1* mutations cause the loss of trichomes on leaves and stems, whereas in roots, they cause the formation of ectopic root hairs (Galway et al., 1994).

Ectopic expression of R in Arabidopsis has the opposite effect: the formation of extra trichomes in stems and leaves (Lloyd et al., 1992, 1994) and a reduction of root hair formation (Galway et al., 1994). Mutation of *ANL2* also affects root architecture, causing the formation of extra cells between the cortex and the epidermis (Kubo et al., 1999). Interestingly, in petunia, *an1* or *an11* mutations do not have a clear effect on the formation of trichomes or root hairs, but they affect seemingly unrelated cellular processes: the acidification of the vacuole and the morphogenesis of the seed coat epidermis (this work).

The vacuole of plant cells plays a central role in pH homeostasis, osmoregulation, ion transport, and the sequestration of (toxic) metabolites (Taiz, 1992). The vacuolar membrane contains ATPase and pyrophosphatase proton pumps that actively acidify the vacuole, whereas the pH of the cytoplasm is kept approximately neutral. The resulting electrochemical gradient serves as a driving force for the uptake of various compounds by transporters and channels in the vacuolar membrane. Despite the physiological importance of vacuolar acidification, little is known about the mechanisms that regulate this process.

Because anthocyanins accumulate in vacuoles and because their absorption spectrum depends on pH, they provide a natural indicator of vacuolar pH (Mol et al., 1998). For example, the change from purple to blue during the development of *Ipomoea* flowers correlates with an increase in vacuolar pH (Yoshida et al., 1995) and requires the Na^+/H^+ exchanger PURPLE (Fukada-Tanaka et al., 2000), which is thought to consume the existing pH gradient, resulting in alkalinization of the vacuolar content.

Petunia flowers normally do not turn blue upon opening, and their vacuolar pH stays on the reddish (low-pH) side of the anthocyanin color spectrum. By genetic analyses, seven loci, designated *PH1* to *PH7*, were identified that mutate to flowers with a more bluish color (de Vlaming et al., 1983; van Houwelingen et al., 1998). Because homogenates prepared from such flowers have higher pH, it is thought that these loci are required for the acidification of the vacuole (de Vlaming et al., 1983). Only one of these *PH* genes has been isolated (*PH6*; Chuck et al., 1993), but because no cDNA clones were isolated, the nature of the gene product remained unknown.

In this article, we show that *AN1*, *AN2*, and *AN11* control, in addition to anthocyanin synthesis, the vacuolar pH in petal cells and the morphology of the seed coat epidermis. Our finding that *ph6* mutants do not define a separate locus, as was thought previously, but represent specific alleles of *AN1* indicates that AN1 controls anthocyanin synthesis and vacuolar pH by distinct mechanisms.

RESULTS

Mutations at *AN1*, *AN2*, and *AN11* Increase the pH of Flower Homogenates

The petunia line W138 arose from the parental line R27 by the insertion of a *dTph1* transposon in the *AN1* gene and bears white flowers with red and pink revertant spots. During the phenotypic analysis of some new *ph* mutants that were identified among W138 progeny, we noticed that the *an1-W138* mutation increased the pH of petal limb homogenates to a similar extent as did mutations in *PH3* and *PH4* (Quattrocchio, 1994). To establish the significance of this observation, we measured the pH of petal limb homogenates for a range of genotypes.

Figure 1 shows that extracts from *an1-W138* homozygous flowers have a pH value that is ~0.7 units higher than flowers homozygous for the *AN1-R27* progenitor allele or from independently isolated *AN1/an1-W138* revertant plants. To determine whether this pH shift is attributable to the absence of anthocyanins, we measured extracts of flowers harboring the unstable *an3-R134* allele.

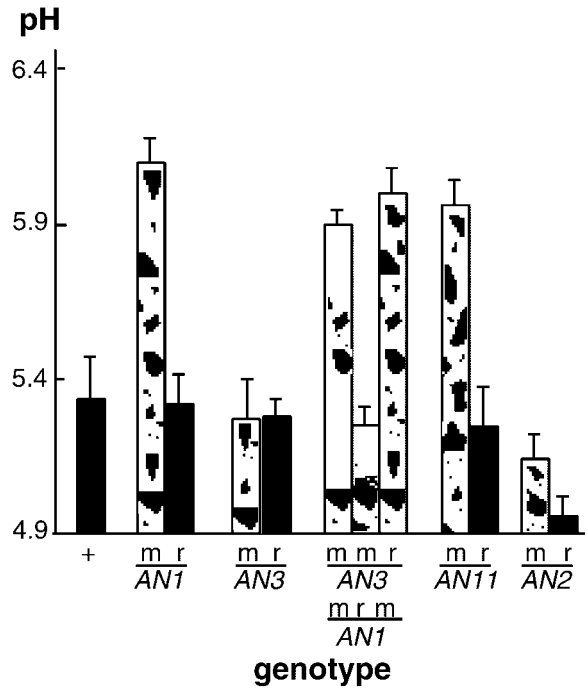

Figure 1. Mutations in Regulatory Anthocyanin Genes Increase the pH of Petal Homogenates.

pH values (means ± SD; $n \geq 4$) were measured in petal homogenates of various genotypes, as indicated on the horizontal axis: +, wild-type allele(s); m, mutable (unstable) alleles; r, derived full-revertant alleles.

AN3 encodes the enzyme flavanone 3β-hydroxylase (F3H), which catalyzes the conversion of flavanones to the corresponding dihydroflavonols, and *an3* mutations block anthocyanin synthesis well before the *an1* block (van Houwelingen et al., 1998). Extracts of *an3-R134* and *AN3* revertant flowers had pH values comparable to that of the wild-type progenitor (R27). Similar results were obtained for mutants containing two other *an3* alleles (*an3-S205* and *an3-S206*; data not shown) and for transgenic plants in which *CHS* genes, which encode chalcone synthase, the first enzyme of flavonoid metabolism, were cosuppressed.

Because the *an3* mutation blocks the anthocyanin pathway at an earlier step than *an1* mutations, *an3* and *an1 an3* double mutants accumulate the same flavonoids (eriodictyol in the R27 background). Even in an *an3* background, the effect of the *an1-W138* mutation on flower extract pH was observed (Figure 1; compare *an1 an3* and *AN1*^{rev}*an3*). Thus, the pH shift observed in *an1-W138* flowers cannot be explained by the absence of anthocyanins.

To determine whether *AN2* and *AN11* also are involved in pH control, we analyzed unstable mutants and revertants for these loci. Flowers harboring the unstable *an11-W137* allele (de Vetten et al., 1997) in the R27 background had an increased pH value similar to that of *an1-W138* flowers, whereas in *AN11* revertant flowers, the pH shifted back to wild-type values (Figure 1). For the *AN2* gene, we measured pH values in the line W82, which harbors an unstable *an2* allele, and used isogenic *AN2* revertants as a control. This showed that the *an2-W82* mutation increased the pH value by 0.3.

Similar results were obtained when we compared pH values in a stable recessive *an2* mutant and isogenic *AN2* plants in which the mutation was complemented by a *35S:AN2* transgene (Quattrocchio et al., 1998). The limited effect of *an2* on anthocyanin synthesis and flower extract pH presumably is caused by the partial redundancy of *AN2* function (Quattrocchio et al., 1998, 1999).

Analysis of Functional AN1 Domains by in Vivo Mutagenesis

To identify functional domains in the AN1 protein, we exploited transposons to generate mutant *an1* alleles by in vivo mutagenesis. The *AN1* gene appears to be a focus for transposon insertions, which enabled us to isolate >30 independent unstable *an1* alleles in random and directed transposon mutagenesis experiments by screening for mutants in which flower pigmentation was altered (van Houwelingen et al., 1998; this work).

We analyzed these unstable *an1* alleles for: (1) molecular alterations in the structure and expression of *an1*, (2) their capacity to drive anthocyanin synthesis and the expression of the structural anthocyanin gene *DFR*, and (3) their capacity to regulate intracellular pH and drive the expression of *PAT1*, a gene of unknown function that is downregulated in *ph4* and *ph3* mutants (F. Quattrocchio, I. Roobeek, W. Verweij, C. Spelt, J. Mol, and R. Koes, unpublished data). The results for the most informative alleles are presented below.

The Wild-Type *AN1* Allele Expresses Distinct mRNA Species That Result from Alternative Polyadenylation

Line R27 bears full-colored (red) flowers with a pH of 5.4 ± 0.1 (Figure 2A) and contains a functional *AN1* gene consisting of nine exons (Figure 3A). RNA gel blot analysis showed that R27 petal limbs contain a major *AN1* mRNA of 2.45 kb (Figure 3B) that encodes a 668–amino acid protein with two well-conserved domains: (1) an ~170–amino acid domain at the N terminus that is conserved in a number of plant bHLH proteins, including R, DEL, and JAF13; and (2) a bHLH domain in the C-terminal half of the protein (Spelt et al., 2000) (Figure 3C). In addition, R27 expresses small amounts of *AN1* transcripts of ~2.9 and ~1.4 kb; the latter transcript was particularly evident in reverse transcriptase–mediated (RT)-PCR products because it is amplified more efficiently than the larger transcripts.

Rapid amplification of cDNA ends (Frohman et al., 1988) showed that the 1.4-kb *an1* transcript resulted from premature polyadenylation in intron 6 and encodes a truncated AN1 protein (Figure 3C). Given that the removal of intron 7 is relatively slow (Spelt et al., 2000), we assume that the 2.9-kb *an1* RNAs represent incompletely spliced transcripts.

an1 Alleles That Disrupt Both Short and Long *AN1* mRNAs

To identify null alleles, we analyzed *an1* alleles with mutations in the 5′ half of the gene, because such mutations affect both the major 2.45-kb mRNA and the minor 1.4-kb mRNA. The unstable allele *an1-Z2309* contains a *dTph1* insertion in exon 1 and represents the most 5′ disruption of the *an1* gene that we found (Figure 3A). RNA analyses showed that *an1-Z2309* flowers are completely devoid of detectable *an1* transcripts (Figure 3B), indicating that it is a null allele. *an1-Z2309* flowers are white (and dotted with red revertant spots) and have a high petal extract pH (Figure 2B), which correlates with a strong reduction of *DFR* and *PAT1* mRNA levels (Figure 3B).

The *an1-W17* allele, which is present in the R27 background, contains an insertion of a novel 3800-bp petunia transposon of the CACTA family, designated *Tph6* (a more detailed characterization of *Tph6* will be published elsewhere), that blocks expression of the wild-type 1.4- and 2.45-kb mRNAs and results in the expression of a 1.3-kb *AN1* mRNA (Figures 3A and 3C). RT-PCR and 3′ rapid amplification of cDNA ends analyses indicated that this RNA arose by premature polyadenylation within *Tph6*, followed by the splicing of exon 2 to a cryptic splice site in *Tph6*; it

Figure 2. Phenotypes of Flowers Harboring Different *an1* Alleles.

Each image shows part of a flower and the pH value of its petal extracts at right (means ± SD; $n \geq 3$). The *an1* alleles present in each flower are indicated in italic type at top. For flowers that are homozygous for an *an1* allele, only a single allele number is given. For flowers that are heterozygous, the numbers of both *an1* alleles are given separated by a slash.

encodes a truncated AN1 protein of 114 amino acids (Figure 3C). Flowers homozygous for *an1-W17* are white (and contain few revertant spots), have a high petal pH (Figure 2C), and express little or no *DFR* and *PAT* mRNA (Figure 3B), indicating that the W17 mutation is similar in effect to *Z2309* and is essentially a null allele.

The Long *AN1* mRNA Is Essential to Direct Anthocyanin Synthesis and Vacuolar Acidification

To assess the contribution of the different AN1 mRNA species to flower pigmentation, we analyzed mutations that specifically affected the accumulation of the long 2.45-kb mRNA. The unstable allele *an1-W138* specifies white flowers with a high petal pH that are dotted with pink and red spots (Figure 2D) as a result of a *dTph1* insertion in the splice acceptor site of exon 7 (Spelt et al., 2000) (Figure 3A). This insertion did not interfere with the expression of the small 1.4-kb *an1* mRNA (which is polyadenylated prematurely at a site upstream of the mutation), but it completely abolished the full-size 2.45-kb *AN1* mRNA. This resulted in a strong reduction of both *DFR* and *PAT1* expression (Figure 3B).

The *dTph1* insertion in *an1-W138* duplicated the acceptor splice of exon 7, and the derived excision alleles contain footprints that contain zero, one, two, or three potential acceptor splice sites at this position (Spelt et al., 2000). Full *AN1* revertants (*an1-W138R*) contain a single splice site that results in the formation of a wild-type amount of the 2.45-kb *AN1* mRNA (Figure 3B) with wild-type sequence (data not shown) (Spelt et al., 2000). By contrast, the excision allele *an1-W225* harbors a 7-bp footprint that contains three potential splice sites. Apparently, most, if not all, of the long *an1* mRNAs are misspliced on one of the alternative splice sites and degraded subsequently, because very low amounts of 2.45-kb *an1* mRNAs were detected in W225

flowers, besides the normal amount of 1.4-kb prematurely polyadenylated transcripts (Figure 3B).

an1-W225 specifies white flowers with an increased petal pH and strongly reduced *DFR* and *PAT1* mRNA levels (Figures 2E and 3B), similar to the null alleles *Z2309* and *W17*. Because *an1-W138* and *an1-W225* still express the 1.4-kb AN1 mRNA but nevertheless have a null phenotype, we infer that the 1.4-kb AN1 mRNA has, at the levels at which it is expressed normally, little or no effect on the synthesis of anthocyanins and vacuolar acidification.

To examine how a reduction of the 2.45-kb *an1* mRNA influenced anthocyanin synthesis and vacuolar acidification, we analyzed the partial revertants of *an1-W138*. Partial revertant alleles of *an1-W138*, such as *an1-X2200*, contain both the original and a potential alternative acceptor splice site (Spelt et al., 2000). RNA analysis showed that *an1-X2200/an1-W138* heterozygous flowers express an amount of 2.45-kb mRNAs that is reduced approximately twofold compared with that expressed by full *AN1/an1-W138* revertants (Figure 3B). Direct sequencing of RT-PCR products showed that these transcripts are an ~1:1 mixture of two mRNAs, one in which exons 6 and 7 are spliced in frame on the original splice site and a second in which exons 6 and 7 are spliced out of frame on the alternative splice site (Figure 3C). Thus, in *X2200* flowers, the amount of wild-type *AN1* mRNA is reduced approximately fourfold.

Interestingly, *an1-X2200* encodes a pink (i.e., light red) flower color, indicating that anthocyanin synthesis is diminished, whereas the pH value is similar to that of wild-type R27 (Figure 2F). Thus, anthocyanin synthesis is affected more strongly by reduced AN1 expression than is vacuolar pH, even though the amount of *DFR* and *PAT* mRNA is reduced equally (approximately twofold).

Mutant *an1* Alleles That Partially Separate the Anthocyanin and pH Function

In the early 1980s, an F2 progeny of two red-flowering petunia lines (family G621) segregated 25% mutants with a purplish flower color. Because these mutants had an increased pH of petal homogenates and complemented mutants for *ph1* to *ph5*, the mutation was assumed to define a new *PH* locus, which was designated *PH6* (P. de Vlaming, unpublished results). Among G621 progeny, a new white-flowering mutant arose, which founded line W160. Allelism tests showed that W160 contained a stable recessive *an1* allele, *an1-W160*; therefore, it was assumed to be an *an1 ph6* double mutant (P. de Vlaming, unpublished data).

More than a decade later, Chuck et al. (1993) generated by mutagenesis with the maize transposon *ACTIVATOR* (*AC*) an unstable *ph* mutation that was allelic to that in W160 and G621 plants and concluded that they had tagged the *PH6* locus. Using this *AC*-tagged *ph6-m1* allele, Chuck et al. (1993) isolated a fragment of the *PH6* gene, but no information on the encoded gene product was provided. However, when we received the sequence of a partial *PH6* cDNA (T. Holton and H. Dooner, unpublished data) during the course of this research, we found to our surprise that it was nearly identical to the sequence that we had determined for *AN1* (Spelt et al., 2000), except for a few sequence alterations that might be attributed to the different lines used for the cDNA cloning.

To determine whether *ph6* mutants represent specific alleles of *AN1*, we analyzed the structure of the *AN1* gene in progeny of the original G621 plants. The progeny of two of these mutants consisted of 34 plants that all bore purplish flowers with red spots (Figure 2G). DNA analysis indicated that they harbored a mutant *an1* allele (*an1-G621*) that contained near the end of exon 6 an insertion of a new 873-bp transposon (Figure 3A) that we designated *dTph5* (details on *dTph5* will be published elsewhere). Molecular analysis of the stable *an1-W160* allele, which arose in G621 progeny, showed that the *dTph5* element had excised and produced an 8-bp footprint that disrupts the AN1 coding sequence (data not shown).

Because these results suggested that the *G621* mutant represents a *dTph5* insertion allele of *AN1*, rather than an allele of a separate *PH6* locus, we performed complementation experiments. Crosses between G621 mutants and null *an1* mutants (*an1-W225* and *an1-W138*) all yielded progeny with a (purplish) *ph* mutant flower color rather than a (red) wild-type color, indicating that the G621 mutation was allelic to *an1* (Figure 2H). Therefore, we concluded that *ph6* mutants do not define a separate locus; rather, they represent particular alleles of *AN1* that lost the control of vacuolar pH but retained the capacity to direct the nearly normal synthesis of anthocyanins. Consistent with this conclusion, *DFR* mRNA expression was reduced approximately twofold in *an1-G621* petals, whereas *PAT1* mRNA was abolished almost completely (Figure 3B). In derived *an1-W160* mutants (Figure 2I), both *DFR* and *PAT1* were downregulated strongly (Figure 3B).

RNA analysis showed that *an1-G621* expresses a 1.4-kb *an1* transcript that is polyadenylated prematurely in the *dTph5* sequence (Figure 3C). This truncated transcript appears to be relatively stable, because it accumulates at threefold higher levels than the wild-type 2.45-kb *an1* mRNA (Figure 3B). By contrast, the excision allele *W160* expresses a reduced amount (~30% of that in the wild-type line R27) of a 2.45-kb mRNA harboring an 8-bp footprint that shifts the reading frame (Figures 3B and 3C).

From the transposon mutagenesis screens, we isolated two additional *an1* alleles, *B3196* and *B2262*, with a strong effect on pH control and a mild effect on anthocyanin synthesis (Figure 2J and data not shown), which is reflected by a mild reduction of *DFR* mRNA and an almost complete reduction of *PAT1* mRNA (Figure 3B). *B2262* and *B3196* contain a *dTph1* insertion in exon 6 in the inverted orientation (Figure 3A and data not shown). This results in premature polyadenylation of the *an1* mRNA in *dTph1* sequences and the formation of a small amount of mRNAs encoding a truncated AN1 protein (Figures 3B and 3C). The *AC*-induced

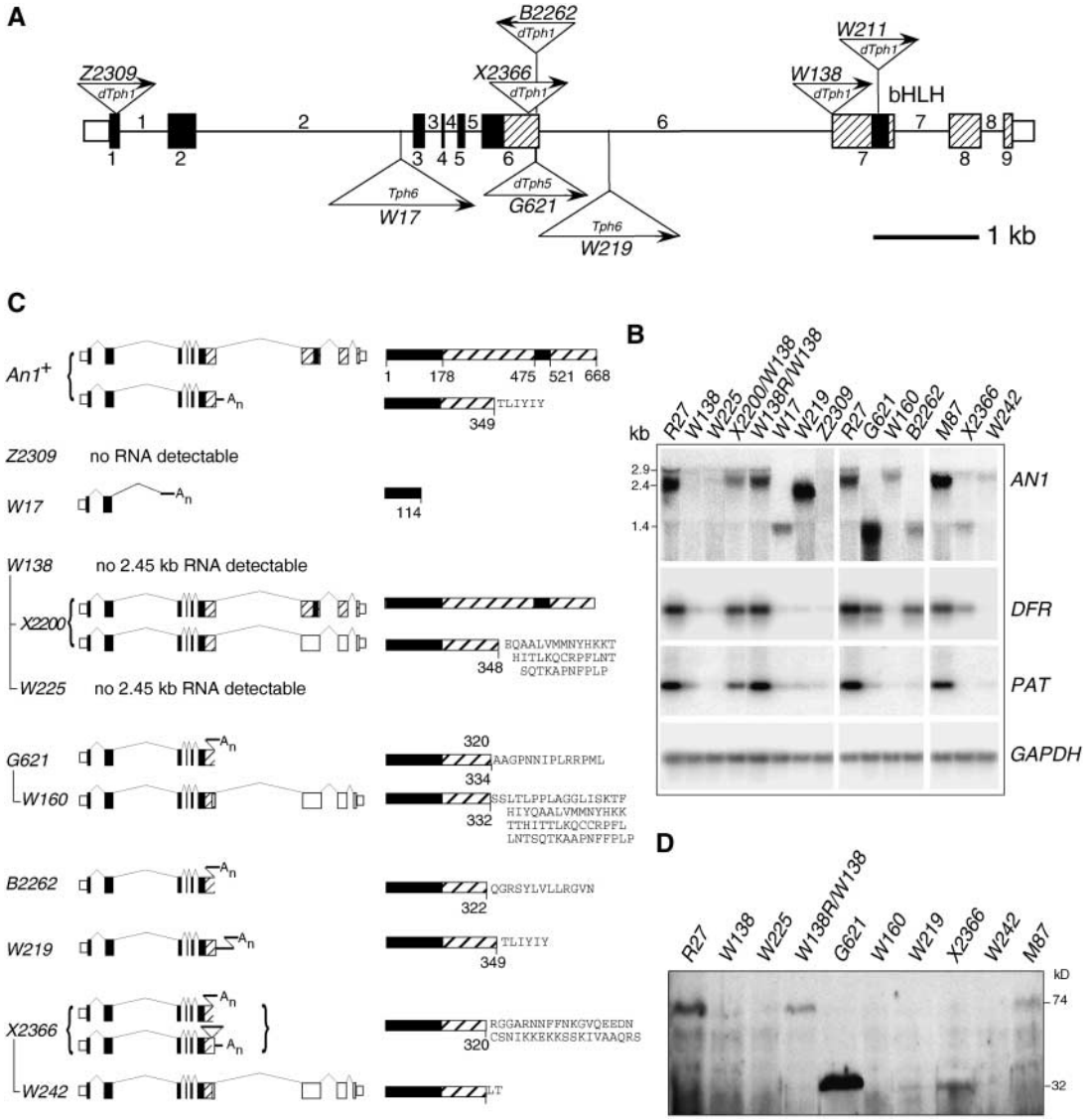

Figure 3. Molecular Analysis of *an1* Alleles.

(A) Structure of the *AN1* gene and mutant alleles. Exons are indicated by rectangles, and introns are indicated by a horizontal line. Exonic regions that encode the conserved N-terminal domain of AN1 and the bHLH region are shaded black; regions encoding less conserved parts of AN1 are indicated by hatching. Exon regions that are not translated are indicated by rectangles of half the height. Triangles (not drawn to scale) denote transposon insertions in the indicated alleles; their orientations are indicated with arrows (arrows pointing right indicate that the orientation of the transposon relative to *AN1* is the same as the sequences in the corresponding GenBank accessions).

(B) Analysis of RNAs expressed in *AN1* and *an1* flowers. RNAs of several genes (indicated at right) were detected by RNA gel blot analysis (*AN1* mRNA) or RT-PCR (*DFR*, *PAT*, and *GAPDH* mRNA). For all alleles (indicated above the lanes) homozygous flowers were used, except for *X2200* and *W138R*, which were heterozygous over the parental *W138* allele.

(C) Structure of mRNAs and proteins expressed by *an1* alleles. The numbers of the alleles are indicated at left, the structure of their mRNAs are indicated in the middle and the encoded proteins are indicated at right. Exons and transposon sequences are drawn as in **(A)**; protein-coding sequences that are not translated in the mutant mRNA are shaded white. The mRNA splicing patterns are indicated by thin lines. The lines connecting the allele numbers indicate how distinct excision alleles derived from the original transposon insertion alleles.

(D) Gel blot analysis of AN1 proteins expressed in *an1* mutants. The flowers analyzed were homozygous for the alleles indicated above the lanes, except for *W138R*, which was heterozygous over the parental mutable allele *W138*.

ph6-m1 allele also expresses a truncated transcript, but its structure and the sequence of the encoded protein are not known (Chuck et al., 1993).

Mutations That Truncate *an1* mRNA and Reduce Both Anthocyanin Synthesis and Vacuolar Acidification

Among the *an1* alleles isolated were several in which the AN1 coding sequence was truncated at a similar point as in the *ph6* alleles but that nevertheless resulted in a strong reduction of anthocyanin synthesis. The allele *an1-W219* had been isolated in progeny of W17 and encodes white flowers with red spots and an increased petal pH (Figure 2K). DNA analyses showed that *an1-W219* contains a *Tph6* insertion in intron 6 (Figure 3A), suggesting that it arose from *an1-W17* by intragenic transposition. *an1-W219* petals contain *an1* transcripts of ~2.1 kb that result from premature polyadenylation within *Tph6* and that encode a truncated protein (Figures 3B and 3C).

Among the progeny of line M87 (Figure 2L), we found the unstable allele *an1-X2366* containing a *dTph1* insertion in exon 6 (Figure 3A). *an1-X2366* clearly is not a null allele, because the flowers have a "blush" of variable intensity, dotted with full-colored revertant spots (Figure 2M). This incomplete block in anthocyanin synthesis is reflected by the relatively large amount of residual *DFR* mRNAs in *X2366* homozygous flowers.

Strikingly, the *X2366* mutation has a much stronger effect on *PAT1* expression, because *PAT1* mRNA is abolished almost completely (Figure 3B). *X2366* petals express a small amount (~20% of the amount in the isogenic wild-type line M87) of two truncated *an1* transcripts that result from premature polyadenylation at two different sites: one in the *dTph1* element and a site downstream of *dTph1* within the intron. Both mRNAs encode an identical 345–amino acid protein (Figure 3C).

Excision of *dTph1* from *X2366* produced a stable recessive allele, *an1-W242*, that is stronger than the parental *X2366* allele, because it encodes completely white flowers with a slightly higher petal pH (Figure 2N) and a complete reduction of both *DFR* and *PAT1* expression (Figure 3B). *an1-W242* expresses a small amount of full-size *an1* transcript (~10% of the amount in the isogenic $An1^+$ line M87) (Figure 3B) that, as a result of the frameshift caused by the 7-bp footprint, encodes a truncated protein of 322 amino acids (Figure 3C).

Analysis of Mutant AN1 Proteins

Among the *an1* alleles isolated were several that contained mutations that truncated the C-terminal end of AN1 in approximately the same region. These alleles all fail to drive vacuolar acidification and expression of *PAT1* but show extensive differences in their capacity to activate anthocyanin synthesis and DFR expression in the order (from high to low): *G621/B2262* > *X2366* > *W219/W160/W242*. To solve this apparent discrepancy, we raised antibodies to AN1 and analyzed the AN1 proteins that accumulated in the mutants.

On protein blots, the anti-AN1 serum detected several bands (Figure 3D). The ~74-kD protein detected in *AN1* petals of R27, M87, and a full-colored revertant of W138 is the AN1 protein, because it is of the expected size and because this protein is missing in all *an1* mutants. The other bands that were detected in these *AN1* lines are not derived from *AN1*, because they were detected in all mutants, including those that lack *AN1* mRNA.

In *an1-G621* petals, we detected a new 32-kD protein, a size expected on the basis of the *an1-G621* mRNA sequence (Figure 3D). Apparently, this mutant AN1 protein is very stable, because it is accumulated at ~30-fold higher levels than wild-type AN1. A similarly sized protein was detected in *X2366* and *W219* petals, but at much lower levels (~1-fold and 0.1-fold the amount of wild-type protein), but not in *W242* and *W160* petals (Figure 3D). Thus, the different capacities of these *an1* alleles to induce anthocyanin synthesis and *DFR* expression, which is in the order *G621* > *X2366* > *W219* > *W160/W242*, correlate perfectly with the amounts of truncated AN1 protein that are accumulated in petal cells.

Transient Expression of *an1* Alleles

Because the protein analyses described above indicated that the different effects on anthocyanin synthesis of the mutant proteins G621 and X2366 are caused by differences in the stability (and hence the steady state levels) of these truncated proteins, rather than by differences in specific activity, we suspected that in vivo the AN1-G621 protein has a reduced capacity to activate anthocyanin synthesis that is compensated for by its ~30-fold overaccumulation.

To reduce the contribution of the high protein stability and the consequent high protein levels to the activities that are measured, we expressed mutant *an1* alleles from the strong and nearly constitutive 35S promoter of *Cauliflower mosaic virus* and assayed the activation of the *DFR* promoter in transient expression assays. The rationale behind these experiments is that the 35S promoter causes strong expression of all alleles, whereas the short time span of the experiment (24 h, compared with several days for the development of a mature flower on the plant) reduces the large differences in protein levels that result from differences in protein stability.

To generate 35S-driven gene constructs for distinct *an1* alleles, we placed cDNA fragments amplified from mutant petals between the 35S promoter and the 3′ end of the *NOPALINE SYNTHASE* gene (see Methods). Each construct was introduced into leaf cells, in combination with a 35S-driven *AN2* gene (*35S*:*AN2*), a *LUCIFERASE* reporter gene driven by the *DFR* promoter (*DFR*:*LUC*), and a constitutively

expressed control gene (*35S*:*β-GLUCURONIDASE*) to correct for variations in transformation efficiency.

Figure 4 shows that coexpression of AN1 and AN2 strongly induced *DFR*:*LUC* expression in leaf cells, whereas either factor alone did not, consistent with previous results (Quattrocchio et al., 1998, 1999; Spelt et al., 2000). When we expressed, instead of the wild-type *AN1* mRNA, the truncated mRNA encoded by *an1-G621*, the induction of *DFR*:*LUC* diminished ~10-fold, indicating that AN1-G621 induces the *DFR* promoter less efficiently than wild-type AN1 does. Expression of AN1-X2366 induced the *DFR* promoter even more weakly, whereas AN1-W160 had no detectable activity at all.

These results indicate that AN1-G621 has a reduced capacity to induce the *DFR* promoter, which in vivo apparently is compensated for by the ~30-fold overexpression of the protein, resulting in nearly normal *DFR* mRNA expression levels.

An Allelic Series Resulting from Alterations in the bHLH Domain

To assess the importance of the bHLH domain for AN1 function in greater detail, we exploited transposon insertions in the region encoding this domain. Among the many new pigmentation mutants found in W138 progeny were several that specified a reduced number of revertant spots that was clearly different from the pattern seen in the W138 parent. Genetic evidence (i.e., the segregation of spotting patterns in the original families and the results from allelism tests) showed that these new phenotypes were attributable to the intragenic transposition of the *dTph1* insertion in the *an1-W138* allele.

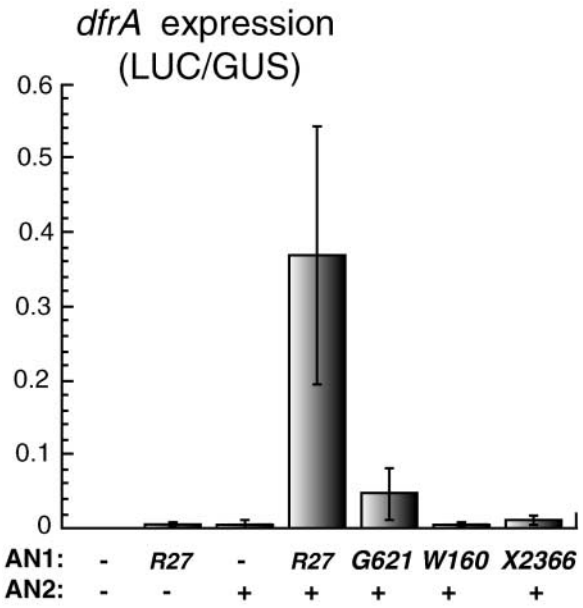

Figure 4. Transient Expression Assays of Mutant *an1* Alleles.

The bars denote luciferase (LUC) activity expressed from a *DFR*:*LUC* reporter gene, normalized for β-glucuronidase (GUS) activity expressed from a codelivered *35S*:*GUS* gene (means ± SE; $n = 5$) in particle-bombarded leaves. Both reporters were codelivered with effector genes expressing AN2 and different mutant AN1 proteins from the 35S promoter, as indicated on the horizontal axis. A minus sign indicates that the corresponding effector was omitted.

PCR and sequence analyses of one of these alleles, *an1-W211*, showed that the *dTph1* element had excised from the original position at the border of intron 6 and exon 7 and created a footprint that would have restored *an1* function (Figure 2T) if a *dTph1* insertion had not disrupted the region encoding the first helix of the bHLH domain. This bHLH insertion apparently creates a null allele, because *an1-W211* homozygous petal limbs lack anthocyanins, have increased pH (Figure 2O), and do not express *DFR* and *PAT1* mRNA (Figure 5).

Somatic and germinal excisions of *dTph1* from *an1-W211* produced a series of four new stable *an1* alleles with activities ranging from null to nearly wild type (Figures 2P to 2S). The *an1-W211W* allele specifies white flowers that completely lack *DFR* and *PAT* mRNA and a petal homogenate pH that is increased by 0.6 (Figure 2P), indicating that this is a null allele. PCR and sequence analysis showed that this allele contains a 7-bp footprint that results in a shift of the AN1 reading frame. The *an1-W211R3* allele has some remaining activity and specifies light pink flowers in which the amount of *DFR* and *PAT* mRNA is reduced strongly (to 10% of the wild-type level); it also produces homogenates in which the pH is increased by 0.4 (Figures 2Q and 5B).

DNA analysis showed that *an1-W211R3* arose from *an1-W211* by excision of the *dTph1* element, which resulted in the formation of a 9-bp footprint and the insertion of three amino acids in the bHLH domain (Figure 5A). The allele *an1-W211R2* specifies pink flowers that contain 20% *DFR* mRNA (relative to the wild type) and produce extracts in which the pH is increased by 0.2 (Figure 2R). PCR and sequence analysis showed that this allele contained a 6-bp footprint resulting in the insertion of two amino acids in AN1. The *an1-W211R1* allele, which specifies dark pink flowers with wild-type pH (Figure 2S) and nearly wild-type levels of *DFR* mRNA (~70% of the amount in the wild type), contains a 3-bp footprint resulting in the insertion of one extra amino acid in AN1 (Figures 5A and 5B).

RNA gel blot analyses (Figure 5C), RT-PCR experiments (data not shown), and protein gel blot experiments (Figure 5D) showed that the three in-frame excision alleles (*W211R1*, *W211R2*, and *W211R3*) all produce wild-type amounts of *an1* mRNA and AN1 protein, indicating that the different phenotypes result from a differences in the activity, not the amount, of the encoded AN1 protein. The *dTph1* insertion in *an1-W211* and the derived frameshift in *an1-W211W* result in strongly reduced amounts of *an1* mRNA and AN1 protein, which explains why these are null alleles.

Regulatory Anthocyanin Genes Control Cell Shape in the Seed Coat

Earlier work indicated that *AN1* controls the coloration not only of floral organs but also of seeds (Chuck et al., 1993; Quattrocchio et al., 1993). However, we noticed that the *an1* and *an11* seed coats also were more fragile (i.e., they tear and fall off regularly) than those of the wild type. To determine the reason for this, we subjected seeds to scanning electron microscopy.

Figure 6A shows that the seed coat epidermis of mature wild-type seeds has a brown color and consists of relatively large cells with a rough, "bubbly" surface and thick, serrated crests where they are attached to neighboring cells. These cells derive from the outer layer of the single petunia integument, which is formed during ovule development, by an extensive differentiation process that involves cell enlargement and thickening of tangential walls (Colombo et al., 1997). However, the epidermal cells do not appear to divide during seed development, because the circumferences of mature seeds and unfertilized ovules contain a similar number of cells (Figure 6B).

The seed coat epidermis of *an1* seeds has a very different morphology: it is yellow and consists of relatively small cells that have a smooth surface and thinner, less serrated crests (Figure 6C). Because the reduced cell size is compensated for by an increase in cell number, *an1* seeds are enclosed within a complete epidermis. Analysis of *an1* ovules showed that the epidermis of the integument contained a similar number of cells than that of wild-type ovules (Figure 6D). This finding is consistent with expression data showing that *AN1* is expressed in the integument endothelium but not in the epidermis (C. Spelt, M. Bliek, and R. Koes, unpublished data). Thus, the supernumerary cells in *an1* seed coats arise from cell divisions that occur after fertilization, during development of the seed.

To determine whether AN1 acts cell autonomously during seed coat development, we analyzed seeds from unstable mutants. The epidermis of *W138* seeds (and other unstable *an1* mutants) mostly consists of small yellow cells, but some seeds contain patches of revertant cells with a wild-type phenotype (Figure 6E). At the borders of revertant sectors, the relatively large *AN1* cells contact a larger than usual number of the much smaller neighboring mutant cells (Figure 6C). The crest between *AN1* and *an1* cells seems to consist of two halves with a wild-type and a mutant appearance, respectively, and crests between *an1* cells have a mutant phenotype even when they contact an AN1 revertant cell on one end. Thus, the role of AN1 during the morphogenesis of seed coat cells is highly cell autonomous.

Seed coats of an *an11* line had the same morphology as *an1* seeds, whereas seed coats of *an2*, *an4*, and *an2 an4* double mutants had a wild-type morphology (data not shown). Given the restricted expression domains of *AN2* and *AN4*, it is possible that seed coat morphogenesis requires a distinct member of this gene family.

To determine whether the altered morphology of *an1* and *an11* seeds is caused by the block in flavonoid synthesis, we analyzed seeds in which the expression of flavonoid biosynthetic enzymes is blocked by either mutation or cosuppression. The epidermis of *an3* seeds has a yellow color that apparently is caused by the absence of flavonoid pigments, but the size and the structure of the cells are similar to those of the wild type (Figure 6F). Similar results were obtained for seed coats of petunia lines in which the expression of *CHS* was blocked by cosuppression (data not shown). Thus, the altered morphology of *an1* and *an11* seed coat cells cannot be explained by the absence of flavonoid compounds.

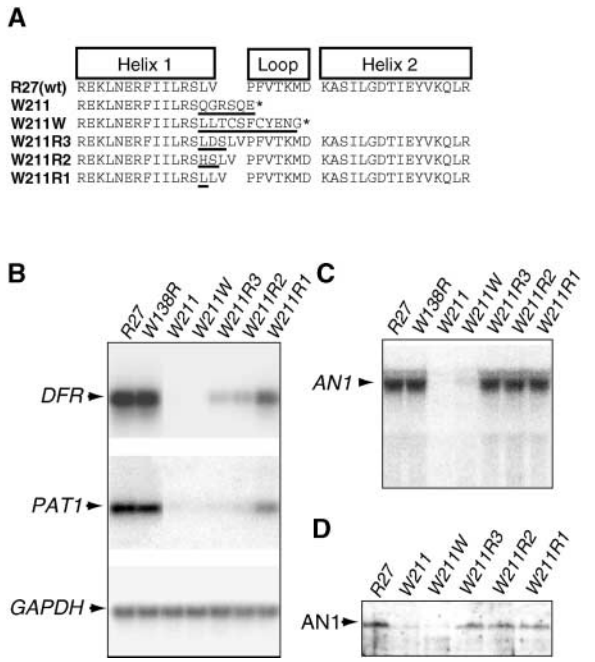

Figure 5. Molecular Analysis of bHLH Domain Mutants of AN1.

(A) Sequences of the bHLH domains encoded by the wild-type (wt) allele *R27*, the transposon insertion allele *W211*, and derived excision alleles (*W211R1* to *W221W*). Regions in which the protein differs from the wild type are underlined. The asterisk denotes the end of the protein.

(B) RT-PCR analysis of mRNAs expressed from the *AN1*-controlled genes *DFR* and *PAT1* and a housekeeping gene (*GAPDH*) in the corolla limbs of *an1* mutants. The analyzed corolla limbs were homozygous for alleles *R27* and *W211*. Alleles *W211W* to *W211R3* were heterozygous over the parental mutable allele *W211*, whereas the full revertant allele, *W138R*, was heterozygous over the parental allele *W138*.

(C) Analysis of the *an1* transcripts expressed in the corolla limbs described in **(B)**. The arrowhead indicates the wild-type 2.45-kb *AN1* mRNA.

(D) Gel blot analysis of AN1 proteins expressed in corolla limbs of the mutants described in **(B)**.

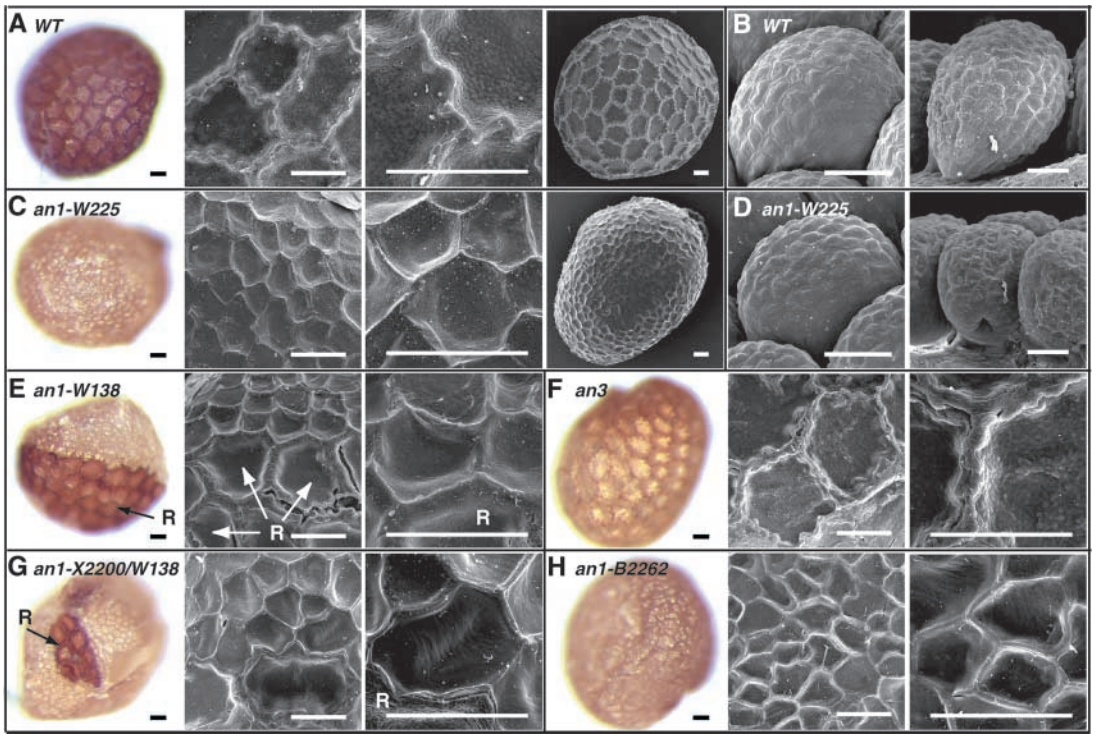

Figure 6. Effect of *an1* Mutations on the Morphology of Seed Coat Cells.

(A) Seed coats of the wild-type (WT) line R27.
(B) Ovules of the wild-type (WT) line R27.
(C) Seed coats of line W225, which is homozygous for the stable null allele *an1-W225*.
(D) Ovules of line W225 (*an1-W225*).
(E) Seed coats of line W138, which is homozygous for the mutable allele *an1-W138*. Note the large revertant sector of large brown seed coat cells (marked R) at left. Revertant cells in the scanning electron micrographs (middle and right) are marked R.
(F) Seed coats of line W234, which is homozygous for a wild-type *AN1* allele and a stable recessive *an3* allele (*an3-W1006*) containing a large deletion (van Houwelingen et al., 1998).
(G) Seed coats of a plant heterozygous for the intermediate allele *X2200* and the mutable allele *W138*. Revertant cells are indicated with R.
(H) Seed coats of a plant homozygous for *an1-B2262*.
The color photographs show untreated mature seeds, and the black-and-white images are scanning electron micrographs. Bars = 50 μm.

To determine whether the AN1 domains involved in the specification of seed coat morphology were separable from those regulating vacuolar pH or anthocyanin synthesis, we analyzed the seed coats from various *an1* mutants. Plants heterozygous for the *an1* alleles *X2200* and *W138* express, in petals, an approximately fourfold reduced amount of wild-type *an1* mRNA. The seed coats of such plants, however, appear fully mutant, because they consist of small yellow cells with occasional patches of revertant cells, which presumably result from reversion of the W138 allele (Figure 6G). Also, seeds that are homozygous for *an1-B2262* or *an1-G621*, alleles that strongly affect *PAT* expression and pH control but that have little or no effect on *DFR* expression and anthocyanin synthesis, appear to have a full mutant phenotype (Figure 6H).

DISCUSSION

In this article, we show that AN1 of petunia acts on at least two and possibly more pathways: the well-defined anthocyanin biosynthesis pathway, and one or more poorly defined pathways involved in the acidification of the vacuole and the morphogenesis of the seed coat epidermis.

Control of Intracellular pH

In *an1*, *an2*, and *an11* petals, the loss of anthocyanin pigments is associated with an increase in vacuolar pH. Because inactivation of enzymes of the anthocyanin pathway,

such as F3H (in *an3* mutants) or CHS (in cosuppressed lines), affects anthocyanin synthesis but not vacuolar pH, it is unlikely that anthocyanins have an effect on the pH or buffering capacity of the vacuole. On the basis of this result, and the finding that some *an1* mutations (alleles previously known as *ph6*) differentially affect anthocyanin synthesis and vacuolar pH, we hypothesize that the effect of *AN1* (and *AN2* and *AN11*) on anthocyanin synthesis and vacuolar pH is mediated by distinct pathways.

AN1 is required for the expression of genes that encode at least eight different enzymes of the anthocyanin pathway (reviewed by Mol et al., 1998) and the glutathione *S*-transferase AN9, which is thought to play a role in the uptake of anthocyanins into the vacuole (Alfenito et al., 1998). Because *AN1* controls pigmentation in a cell-autonomous manner but *AN9* does not, it is thought that *AN1* controls the expression of a protein that acts after AN9, possibly the pump that transports the anthocyanin into the vacuole (Alfenito et al., 1998). If this is the case, it would explain why full AN1 revertant spots on weakly colored flowers are surrounded by a "halo" of white anthocyaninless cells (Figure 2F).

High anthocyanin pumping activity in the revertant cells would result in rapid vacuolar sequestration of anthocyanins, including those that arrive by diffusion from neighboring mutant cells with weak AN1 and pump activity, resulting in depletion of anthocyanins in those cells. Consistent with this idea, the halos are several cells wide (large revertant sectors have wider halos than small revertant spots) and have a sharp inner edge with white cells neighboring the full-colored revertant cells, whereas the outer edge consists of a gradient of cells with colors ranging from white to the normal mutant color. If this idea is true, it suggests that the unknown transporter also is downregulated in *an1-G621* and *ph6-m1* mutants, because *An1*$^+$ revertant spots on such flowers also are surrounded by a white halo (Figures 2G and 2H) (Chuck et al., 1993).

To date, two different transporters have been implicated in the transport of flavonoids: (1) the MATE-type (for multidrug and toxic compound extrusion) protein TT12, which is required for vacuolar localization of proanthocyanidins in the Arabidopsis seed coat (Debeaujon et al., 2001), and (2) two MRP-type (for multidrug-related protein) glutathione pumps that could transport anthocyanins when expressed in yeast (Lu et al., 1997). However, because it is not known whether these transporters translocate protons and whether their expression is controlled by *TT8*, the Arabidopsis *AN1* homolog (Nesi et al., 2000), it remains to be determined whether anthocyanin transport and vacuolar acidification are linked directly.

Two genes have been identified that are coregulated by *AN1* and one or more *PH* genes. One of them, *MYB27*, encodes a MYB domain protein of unknown function that is regulated by AN1 and PH4 (Mur, 1995; Spelt et al., 2000). The gene used in this study, *PAT1*, is downregulated in *an1*, *an11*, *ph3*, and *ph4* mutants (F. Quattrocchio, I. Roobeek, W. Verweij, C. Spelt, J. Mol, and R. Koes, unpublished data) as well as in *an1* mutants with specific defects in pH control (Figure 3B), suggesting that it operates in an *AN1*/*PH3*/*PH4*-controlled pH pathway. The further elucidation of this pathway will have to await the characterization of *PAT1* and the identification of additional genes that function in the same pathway.

Control of Seed Coat Cell Morphology

Earlier work indicated that *AN1* controls the coloration not only of floral organs but also of seeds (Chuck et al., 1993; Quattrocchio et al., 1993). The color of the seed coat epidermis depends on a flavonoid-derived pigment, presumably a proanthocyanidin, that requires the activity of enzymes such as CHS, F3H/AN3, and DFR (Figure 6) (Koes et al., 1990; Quattrocchio et al., 1993), similar to the situation in Arabidopsis (Debeaujon et al., 2000; Sagasser et al., 2002). Because ovules are uncolored, the synthesis of this pigment occurs after fertilization and coincides with a strong increase of DFR expression (Huits et al., 1994). Strikingly, *AN1* and *AN11* affect not only the color but also the morphogenesis of cells in the seed coat epidermis (Figure 6).

After fertilization, the seed increases severalfold in size, which requires that the epidermis extends proportionally. This extension seems primarily the result of cell expansion, not cell division, because the epidermis of the ovule integument and the mature seed coat consist of a similar number of cells (Figure 6). Cell expansion is accompanied by other morphological changes, such as extensive thickening of the cell wall and formation of starch granules (Colombo et al., 1997; Western et al., 2000; Windsor et al., 2000). One or more of these processes appears to be disrupted in *an1* (and *an11*) seeds, because their epidermis consists of an increased number of smaller cells.

At least two explanations can account for this phenotype, and they are not mutually exclusive. First, the primary role of AN1 may be to prevent the growing epidermal cells from undergoing cell division. Alternatively, the primary role of AN1 may be in cell enlargement, and the induction of cell division in *an1* seeds may be a secondary effect that is induced indirectly, for instance, by the more rapid expansion of underlying cell layers.

Although the mechanism by which AN1 controls seed coat development is unclear, some possibilities can be excluded. First, alterations in the flavonoid metabolism of *an1* seeds cannot account for the observed morphological changes, because these are not seen in seeds in which the expression of the enzyme F3H (*an3* mutants) or CHS (cosuppressed lines) is blocked. The synthesis of flavonoid (polymers) apparently is not required for the enlargement of these epidermal cells or for the thickening of their walls, because these processes show little or no alterations in *an3* mutants or *chs* cosuppressed lines.

Because the mutations *an1-G621* and *an1-B2262*, which in the flower primarily affect vacuolar acidification, have

strong effects on the size and shape of seed coat cells, one may argue that this is an indirect result of the misregulation of vacuolar pH. However, we consider this possibility unlikely, because the seed coats of the known *ph* mutants consist of cells of nearly normal size and shape, even though some of the mutations affect seed color. Therefore, we favor the hypothesis that *AN1* may control a third set of genes, in addition to those involved in anthocyanin synthesis and pH control, that is required for the normal morphology of seed coat cells.

Role of the bHLH Domain

In mammalian transcription factors, the bHLH domain enables these proteins to form homodimers and heterodimers through the HLH domain and to contact DNA through the basic domain (Massari and Murre, 2000). Although its conservation indicates an equally important role for the bHLH domain in plant proteins, its precise function remains unclear.

Transient expression experiments showed that deletion of the bHLH domain of B or R diminished the transcriptional activation of the *BRONZE1* target promoter by only 50%, suggesting that the bHLH domain has a marginal role (Goff et al., 1992; Liu et al., 1998). By contrast, insertions of two, three, or seven amino acids into the bHLH region abolished the transcriptional activation of anthocyanin genes almost completely, in vivo as well as in transient expression assays, even though protein stability and nuclear import were unaffected (Liu et al., 1998). Although it remains unclear why deletion of the bHLH domain had less effect on the activity of R/B than small insertions, this finding raises the question of why the bHLH domain has been conserved over such a long period of evolution.

Mutational analyses of AN1, which is functionally and evolutionarily distinct from but structurally related to R, shed more light on this issue. Insertions of one, two, or three amino acids into the AN1 bHLH domain (as in the mutants *W211R1* to *W211R3*) result in a progressive reduction of the capacity (but not in the amount) of AN1 to induce the expression of *PAT1* and *DFR* and to drive anthocyanin synthesis and vacuolar acidification. This indicates that the bHLH domain is involved in the activation of anthocyanin synthesis and vacuolar acidification.

The removal of the C-terminal half of AN1, including the bHLH domain, while the amount of AN1 is kept approximately normal (as in *an1-X2366* mutants) reduces anthocyanin synthesis and DFR expression strongly (to approximately the same extent as the insertion of two or three amino acids in the HLH region), but not completely. Although this result seems to indicate that AN1 is more sensitive to C-terminal deletions than is R or B, this is not certain. First, we cannot exclude the possibility that the transcription activation capacity of AN1-X2366 is underestimated as a result of difficulties with nuclear import. Second, because the bHLH deletion derivatives of R and B were analyzed in transient assays only, the stability and the specific activity of mutant R/B proteins are unknown.

Strikingly, removal of the C-terminal part of AN1 affects vacuolar acidification, seed coat morphogenesis, and PAT1 expression much stronger than anthocyanin synthesis or DFR expression. When overexpressed at levels ~30-fold higher than those in the wild type (as in *an1-G621* mutants), such a truncated AN1 protein drives nearly normal levels of DFR expression and anthocyanin synthesis but cannot drive vacuolar acidification, seed coat morphogenesis, or *PAT1* expression.

This fact indicates that the C-terminal region of AN1, including the bHLH domain, plays a more prominent role in vacuolar acidification and seed coat morphogenesis than it does in anthocyanin synthesis, which may be the reason for the evolutionary conservation of this domain. Whether this is because AN1 regulates these different processes by interactions with different protein partners or via different *cis*-acting elements in the target gene promoters is the subject of further research.

Evolutionary Aspects

Based on comparative studies in petunia and maize (Quattrocchio et al., 1993, 1998, 1999) and the strong conservation of the WD repeat protein AN11 even in animals and yeast (de Vetten et al., 1997), we speculated that when the anthocyanin pathway arose during evolution, the newborn structural genes were linked to preexisting regulators, the ancestors of the Arabidopsis, petunia, and maize regulators that are studied today (Koes et al., 1994). The original function of the anthocyanin regulators has remained elusive, however. Whether one or more of the additional functions of anthocyanin regulators that have been revealed in Arabidopsis and petunia represents the hypothetical ancient function is difficult to determine, especially because these additional functions do not appear to be as widespread among plant species as anthocyanin synthesis.

In Arabidopsis, TTG controls hair cell fate by interaction with MYB proteins (GLABROUS1 [GL1] and WEREWOLF [WER]; Lee and Schiefelbein, 1999, 2001) and bHLH proteins (GL3; Payne et al., 2000) that are distinct from the anthocyanin-specific MYB (TT2, PAP1, and PAP2) and bHLH (TT8) proteins. Moreover, the genetic and physical interactions between TTG, GL1, WER, and GL3 (reviewed by Szymanski et al., 2000) closely resemble those between the anthocyanin regulators AN1, AN2, AN11, and JAF13 (A. Kroon and R. Koes, unpublished data) and C1 and B (Goff et al., 1992). This finding indicates that the mechanisms that specify hair cell fate in Arabidopsis are essentially similar to the mechanisms that drive anthocyanin synthesis in a wide variety of species.

However, the multicellular trichomes of Solanaceae appear to be specified by regulators that are distinct from those that specify the fate of the unicellular Arabidopsis

hairs. First, neither mutations nor ectopic overexpression of AN1, AN2, and AN11 results in an obvious trichome phenotype (Quattrocchio et al., 1998; Spelt et al., 2000; this paper). Given that AN11 is a single gene in petunia (de Vetten et al., 1997), it is unlikely that the absence of an *an11* trichome phenotype is attributable to genetic redundancy. Second, the ectopic expression of maize R induces trichome formation in Arabidopsis but not in tobacco or petunia (Lloyd et al., 1992; Quattrocchio et al., 1993). Third, trichome formation in tobacco and Arabidopsis involves MYB factors that are distinct from GL1 (Payne et al., 1999). Thus, the role of the WD repeat proteins TTG/AN11 in the specification of hairs appears to be less widespread than their role in anthocyanin synthesis.

Similarly the function of AN1 and AN11 in seed coat morphogenesis appears to be less widespread than their function in anthocyanin synthesis, because mutations in the homologous Arabidopsis genes seem to have little effect on the size and shape of seed coat epidermal cells (Debeaujon et al., 2000). The seed coat defects seen in *tt1* mutants involve the differentiation of the seed coat endothelium (Sagasser et al., 2002), not the epidermis, as in *an1* and *an11* mutants. Whether anthocyanin regulators also control vacuolar acidification in species other than petunia remains unknown, because, to our knowledge, this question has not been analyzed in any other species.

METHODS

Petunia Lines and Mutants

Unless stated otherwise, all mutant lines used in this study were generated in the genetic background of the wild-type *Petunia hybrida* line R27. The alleles *an1-W17* (formerly *an1*$^{s/-+}$) and *an1-W138* (formerly *an1*$^{s/p-+}$) were isolated in progeny of R27 (Bianchi et al., 1978; Doodeman et al., 1984). *an1-W219* was isolated in progeny of *an1-W17* (T. Gerats and P. de Vlaming, unpublished data). The insertion alleles *Z2083*, *B2261*, and *W2175* were identified among progeny of *an1-W138* (van Houwelingen et al., 1998; this work). The excision allele *X2200*, derived from *an1-W138*, has been described previously (Spelt et al., 2000). The insertion alleles *G621* (P. de Vlaming, unpublished data) and *X2366* (van Houwelingen et al., 1998) arose in genetic backgrounds that were not related directly to R27.

Scanning Electron Microscopy

Mature seeds were fixed, critical point dried, and analyzed by scanning electron microscopy as described previously (Souer et al., 1996).

pH of Petal Extracts

The petal limbs of two flowers were ground with a pestle and mortar in 4 mL of distilled water, and the pH of the homogenate was measured immediately (to avoid alkalinization by uptake of atmospheric carbon dioxide) with a normal pH electrode. Although the differences in pH between petal extracts from different genotypes were always reproducible, the actual pH values varied between experiments, probably as a result of variations in environmental conditions. This variation is reflected by the small quantitative differences between the data sets shown in Figures 1 and 2, because these derive from distinct sets of plants grown at different periods.

Molecular Analysis of Mutant *an1* Alleles

To determine the lesions in various mutant *an1* alleles, we first determined the site and the origin of transposon insertions found in various unstable *an1* alleles. Therefore, genomic DNA digested with different combinations of restriction enzymes was subjected to DNA gel blot analysis using fragments of the wild-type locus as a hybridization probe to visualize specific parts of the mutant locus. Once the insertions were mapped approximately, they were amplified by PCR together with the flanking *an1* sequences using primers complementary to *an1* and sequenced directly or first cloned in plasmid vectors and then sequenced. Lesions in derived stable recessive or revertant alleles were analyzed by PCR amplification and sequence analysis of the region surrounding the transposon insertion in the parental allele.

Transient Expression Assays

To generate 35S-driven constructs for distinct *an1* alleles, we amplified, by reverse transcriptase–mediated (RT)-PCR on RNA isolated from petals containing the appropriate mutant *an1* alleles, a cDNA fragment spanning the region from bp 1010 (the position in wild-type cDNA) to the poly(A) tail. RT-PCR products were digested with SacII (which cuts at position 1065) and XhoI (which cuts in the rapid amplification of cDNA ends primer) and used to replace the corresponding region of wild-type *AN1* in the *35S:AN1* construct described by Spelt et al. (2000). The inserts of the resulting *35S*:*an1* constructs were resequenced to exclude PCR errors or cloning artifacts that had occurred.

Details regarding the fusion genes *35S*:*AN2*, *DFR*:*LUCIFERASE*, and *35S*:*β-GLUCURONIDASE* and procedures for the transient transformation of petunia W115 leaves are described elsewhere (de Vetten et al., 1997; Quattrocchio et al., 1998).

RNA Analyses

RNA isolation, RNA gel blot analyses, and RT-PCR were performed as described previously (de Vetten et al., 1997; Quattrocchio et al., 1998; Spelt et al., 2000). RT-PCR products were detected by gel blot hybridization and quantified by phosphor imaging. To analyze mutant *an1* transcripts, they were first examined by RNA gel blot analysis to determine their size and quantity. To determine the structure in greater detail, specific parts of these *an1* transcripts were amplified by PCR using either a combination of two different *an1*-specific primers or one *an1*-specific primer in combination with the 3′ rapid amplification of cDNA ends primer (Frohman et al., 1988). Products that had been amplified with “informative” primer pairs were cloned in plasmid vectors and sequenced or sequenced directly.

Expression of AN1 in *Escherichia coli* and Immunological Methods

Several AN1 protein fragments were expressed in *E. coli* as His_6-tagged fusions and purified on nickel–nitrilotriacetic acid agarose columns (Qiagen, Valencia, CA) as described (de Vetten et al., 1997). One mouse was immunized with an AN1 fragment from amino acids 140 to 390 ($AN_{140-390}$) and a second mouse with a 1:1 mixture of $AN_{140-390}$ and the full AN1 protein as described previously (de Vetten et al., 1997). The protein blots shown in Figures 3D and 5D were made with the first antiserum; the other serum gave essentially the same results, but the background was higher.

Distribution of Biomaterials

Upon request, all novel materials described in this article will be made available in a timely manner for noncommercial research purposes. No restrictions or conditions will be placed on the use of any materials described in this article that would limit their use for noncommercial research purposes.

Accession Numbers

The GenBank accession numbers for the genes mentioned in this article are AF260918 (*AN1*), AF260921 (*Tph6*), and AF260920 (*dTph5*).

ACKNOWLEDGMENTS

We thank Saskia Kars for help with scanning electron microscopy, Daisy Kloos for help with the genetic experiments, and Pieter Hoogeveen and Martina Meesters for their care of the plants.

Received April 9, 2002; accepted June 4, 2002.

REFERENCES

Alfenito, M.R., Souer, E., Goodman, C.D., Buell, R., Mol, J., Koes, R., and Walbot, V. (1998). Functional complementation of anthocyanin sequestration in the vacuole by widely divergent glutathione *S*-transferases. Plant Cell **10,** 1135–1149.

Bianchi, F., Cornelissen, P.J.T., Gerats, A.G.M., and Hogervorst, J.M.W. (1978). Regulation of gene action in *Petunia hybrida*: Unstable alleles of a gene for flower colour. Theor. Appl. Genet. **53,** 157–167.

Borevitz, J.O., Xia, Y., Blount, J., Dixon, R.A., and Lamb, C. (2000). Activation tagging identifies a conserved MYB regulator of phenylpropanoid biosynthesis. Plant Cell **12,** 2383–2394.

Bruce, W., Folkerts, O., Garnaat, C., Crasta, O., Roth, B., and Bowen, B. (2000). Expression profiling of the maize flavonoid pathway genes controlled by estradiol-inducible transcription factors CRC and P. Plant Cell **12,** 65–80.

Chuck, G., Robbins, T., Nijjar, C., Ralston, E., Courtney-Gutterson, N., and Dooner, H.K. (1993). Tagging and cloning of a petunia flower color gene with the maize transposable element *Activator*. Plant Cell **5,** 371–378.

Colombo, L., Franken, J., Van der Krol, A.R., Wittich, P.E., Dons, H.J., and Angenent, G.C. (1997). Downregulation of ovule-specific MADS box genes from petunia results in maternally controlled defects in seed development. Plant Cell **9,** 703–715.

Debeaujon, I., Leon-Kloosterziel, K.M., and Koornneef, M. (2000). Influence of the testa on seed dormancy, germination, and longevity in Arabidopsis. Plant Physiol. **122,** 403–414.

Debeaujon, I., Peeters, A.J., Leon-Kloosterziel, K.M., and Koornneef, M. (2001). The *TRANSPARENT TESTA12* gene of Arabidopsis encodes a multidrug secondary transporter-like protein required for flavonoid sequestration in vacuoles of the seed coat endothelium. Plant Cell **13,** 853–871.

de Vetten, N., Quattrocchio, F., Mol, J., and Koes, R. (1997). The *an11* locus controlling flower pigmentation in petunia encodes a novel WD-repeat protein conserved in yeast, plants and animals. Genes Dev. **11,** 1422–1434.

de Vlaming, P., Schram, A.W., and Wiering, H. (1983). Genes affecting flower colour and pH of flower limb homogenates in *Petunia hybrida*. Theor. Appl. Genet. **66,** 271–278.

Doodeman, M., Boersma, E.A., Koomen, W., and Bianchi, F. (1984). Genetic analysis of instability in *Petunia hybrida*. 1. A highly unstable mutation induced by a transposable element inserted at the *An1* locus for flower colour. Theor. Appl. Genet. **67,** 345–355.

Frohman, M.A., Dush, M.K., and Martin, G.R. (1988). Rapid production of full-length cDNAs from rare transcripts: Amplification using a single gene-specific oligonucleotide primer. Proc. Natl. Acad. Sci. USA **85,** 8998–9002.

Fukada-Tanaka, S., Inagaki, Y., Yamaguchi, T., Saito, N., and Iida, S. (2000). Colour-enhancing protein in blue petals. Nature **407,** 581.

Galway, M.E., Masucci, J.D., Lloyd, A.M., Walbot, V., Davis, R.W., and Schiefelbein, J.W. (1994). The *TTG* gene is required to specify epidermal cell fate and cell patterning in the Arabidopsis root. Dev. Biol. **166,** 740–754.

Goff, S.A., Cone, K.C., and Chandler, V.L. (1992). Functional analysis of the transcription activator encoded by the maize B-gene: Evidence for a direct functional interaction between two classes of regulatory proteins. Genes Dev. **6,** 864–875.

Holton, T.A., and Cornish, E.C. (1995). Genetics and biochemistry of anthocyanin biosynthesis. Plant Cell **7,** 1071–1083.

Huits, H.S.M., Gerats, A.G.M., Kreike, M.M., Mol, J.N.M., and Koes, R.E. (1994). Genetic control of dihydroflavonol 4-reductase gene expression in *Petunia hybrida*. Plant J. **6,** 295–310.

Koes, R.E., Quattrocchio, F., and Mol, J.N.M. (1994). The flavonoid biosynthetic pathway in plants: Function and evolution. Bioessays **16,** 123–132.

Koes, R.E., Van Blokland, R., Quattrocchio, F., Van Tunen, A.J., and Mol, J.N.M. (1990). Chalcone synthase promoters in petunia are active in pigmented and unpigmented cell types. Plant Cell **2,** 379–392.

Kubo, H., Peeters, A.J., Aarts, M.G., Pereira, A., and Koornneef, M. (1999). *ANTHOCYANINLESS2*, a homeobox gene affecting anthocyanin distribution and root development in Arabidopsis. Plant Cell **11,** 1217–1226.

Lee, M.M., and Schiefelbein, J. (1999). WEREWOLF, a MYB-related protein in Arabidopsis, is a position-dependent regulator of epidermal cell patterning. Cell **99,** 473–483.

Lee, M.M., and Schiefelbein, J. (2001). Developmentally distinct

MYB genes encode functionally equivalent proteins in Arabidopsis. Development **128,** 1539–1546.

Liu, Y., Wang, L., Kermicle, J.L., and Wessler, S.R. (1998). Molecular consequences of *Ds* insertion into and excision from the helix-loop-helix domain of the maize *R* gene. Genetics **150,** 1639–1648.

Lloyd, A.M., Schena, M., Walbot, V., and Davis, R. (1994). Epidermal cell fate determination in Arabidopsis: Patterns defined by a steroid-inducible regulator. Science **266,** 436–439.

Lloyd, A.M., Walbot, V., and Davis, R.W. (1992). *Arabidopsis* and *Nicotiana* anthocyanin production activated by maize regulators *R* and *C1*. Science **258,** 1773–1775.

Lu, Y.-P., Li, Z.-S., and Rea, P.A. (1997). *AtMRP1* gene of *Arabidopsis* encodes a glutathione *S*-conjugate pump: Isolation and functional definition of a plant ATP-binding cassette transporter gene. Proc. Natl. Acad. Sci. USA **94,** 8243–8248.

Massari, M.E., and Murre, C. (2000). Helix-loop-helix proteins: Regulators of transcription in eucaryotic organisms. Mol. Cell. Biol. **20,** 429–440.

Mol, J., Grotewold, E., and Koes, R. (1998). How genes paint flowers and seeds. Trends Plant Sci. **3,** 212–217.

Mur, L. (1995). Characterization of Members of the *myb* Gene Family of Transcription Factors from *Petunia hybrida*. PhD dissertation (Amsterdam: Vrije Universiteit).

Nesi, N., Debeaujon, I., Jond, C., Pelletier, G., Caboche, M., and Lepiniec, L. (2000). The *TT8* gene encodes a basic helix-loop-helix domain protein required for expression of DFR and BAN genes in Arabidopsis siliques. Plant Cell **12,** 1863–1878.

Nesi, N., Jond, C., Debeaujon, I., Caboche, M., and Lepiniec, L. (2001). The Arabidopsis *TT2* gene encodes an R2R3 MYB domain protein that acts as a key determinant for proanthocyanidin accumulation in developing seed. Plant Cell **13,** 2099–2114.

Payne, C.T., Zhang, F., and Lloyd, A.M. (2000). *GL3* encodes a bHLH protein that regulates trichome development in Arabidopsis through interaction with GL1 and TTG1. Genetics **156,** 1349–1362.

Payne, T., Clement, J., Arnold, D., and Lloyd, A. (1999). Heterologous myb genes distinct from *GL1* enhance trichome production when overexpressed in *Nicotiana tabacum*. Development **126,** 671–682.

Quattrocchio, F. (1994). Regulatory Genes Controlling Flower Pigmentation in *Petunia hybrida*. PhD thesis (Amsterdam: Vrije Universiteit).

Quattrocchio, F., Wing, J., van der Woude, K., Souer, E., de Vetten, N., Mol, J., and Koes, R. (1999). Molecular analysis of the *anthocyanin2* gene of *Petunia* and its role in the evolution of flower color. Plant Cell **11,** 1433–1444.

Quattrocchio, F., Wing, J.F., Leppen, H.T.C., Mol, J.N.M., and Koes, R.E. (1993). Regulatory genes controlling anthocyanin pigmentation are functionally conserved among plant species and have distinct sets of target genes. Plant Cell **5,** 1497–1512.

Quattrocchio, F., Wing, J.F., van der Woude, K., Mol, J.N.M., and Koes, R. (1998). Analysis of bHLH and MYB-domain proteins: Species-specific regulatory differences are caused by divergent evolution of target anthocyanin genes. Plant J. **13,** 475–488.

Sagasser, M., Lu, G.H., Hahlbrock, K., and Weisshaar, B. (2002). *A. thaliana* TRANSPARENT TESTA 1 is involved in seed coat development and defines the WIP subfamily of plant zinc finger proteins. Genes Dev. **16,** 138–149.

Souer, E., van Houwelingen, A., Kloos, D., Mol, J.N.M., and Koes, R. (1996). The *no apical meristem* gene of petunia is required for pattern formation in embryos and flowers and is expressed at meristem and primordia boundaries. Cell **85,** 159–170.

Spelt, C., Quattrocchio, F., Mol, J., and Koes, R. (2000). *anthocyanin1* of petunia encodes a basic-helix loop helix protein that directly activates structural anthocyanin genes. Plant Cell **12,** 1619–1631.

Szymanski, D.B., Lloyd, A.M., and Marks, M.D. (2000). Progress in the molecular genetic analysis of trichome initiation and morphogenesis in Arabidopsis. Trends Plant Sci. **5,** 214–219.

Taiz, L. (1992). The plant vacuole. J. Exp. Biol. **172,** 113–122.

van Houwelingen, A., Souer, E., Spelt, C., Kloos, D., Mol, J., and Koes, R. (1998). Analysis of flower pigmentation mutants generated by random transposon mutagenesis in *Petunia hybrida*. Plant J. **13,** 39–50.

Walker, A.R., Davison, P.A., Bolognesi-Winfield, A.C., James, C.M., Srinivasan, N., Blundell, T.L., Esch, J.J., Marks, M.D., and Gray, J.C. (1999). The *TRANSPARENT TESTA GLABRA1* locus, which regulates trichome differentiation and anthocyanin biosynthesis in Arabidopsis, encodes a WD40 repeat protein. Plant Cell **11,** 1337–1350.

Western, T.L., Skinner, D.J., and Haughn, G.W. (2000). Differentiation of mucilage secretory cells of the Arabidopsis seed coat. Plant Physiol. **122,** 345–356.

Windsor, J.B., Symonds, V.V., Mendenhall, J., and Lloyd, A.M. (2000). Arabidopsis seed coat development: Morphological differentiation of the outer integument. Plant J. **22,** 483–493.

Winkel-Shirley, B. (2001). Flavonoid biosynthesis: A colorful model for genetics, biochemistry, cell biology, and biotechnology. Plant Physiol. **126,** 485–493.

Yoshida, K., Kondo, T., Okazaki, Y., and Katou, K. (1995). Cause of blue petal colour. Nature **373,** 291.